

## Supporting Information for

# (B,P,Co,Fe)-Ni Modified on Nanowood for Boosting Seawater Urea Electro-Oxidation

Hongjiao Chen<sup>a</sup>, Kewei Zhang<sup>a</sup>, Yanzhi Xia<sup>a</sup>, Jian Li<sup>b</sup>, Bin Hui<sup>a,\*</sup>

<sup>a</sup> State Key Laboratory of Bio-Fibers and Eco-Textiles, Shandong Collaborative Innovation Center of Marine Biobased Fiber and Ecological Textile, Institute of Marine Biobased Materials, School of Materials Science and Engineering, Qingdao University, Qingdao 266071, P.R. China

<sup>b</sup> Key Laboratory of Bio-based Materials Science and Technology of Ministry of Education, Research Center of Wood Bionic Intelligent Science, School of Materials Science and Engineering, Northeast Forestry University, Harbin, 150040, PR China

## Table of Contents

- Fig. S1** SEM image of the natural paulownia wood.
- Fig. S2** SEM images of the natural paulownia wood along the direction of tree growth.
- Fig. S3** The photo of the natural leave loaded with alloys.
- Fig. S4** SEM images of the (B,P,Co,Fe)-Ni@PW.
- Fig. S5** SEM images of the (B,P,Co,Fe)-Ni@PW.
- Fig. S6** XRD pattern of PW.
- Fig. S7** XRD pattern of P-Ni@PW.
- Fig. S8** HRTEM images of (B,P,Co,Fe)-Ni@PW
- Fig. S9** High-resolution XPS spectra of (B,P,Co,Fe)-Ni@PW for C 1s.
- Fig. S10** High-resolution XPS spectra of (P,Co)-Ni@PW and (B,P,Co,Fe)-Ni@PW for O 1s.
- Fig. S11** Nyquist plots of the (B,P,Co,Fe)-Ni@PW for OER and UOR.
- Fig. S12** Nyquist plots of the (B,P,Co,Fe)-Ni@PW for HER in 1 M KOH with and without urea.
- Fig. S13** HER polarization curves of (B,P,Co,Fe)-Ni@PW with different mass ratios.
- Fig. S14** UOR polarization curves of (B,P,Co,Fe)-Ni@PW with different mass ratios.
- Fig. S15** HER polarization curves of (B,P,Co,Fe)-Ni@PW with different mass ratios.
- Fig. S16** UOR polarization curves of (B,P,Co,Fe)-Ni@PW with different mass ratios.
- Fig. S17** HER polarization curves of (B,P,Co,Fe)-Ni@PW at different reaction times.
- Fig. S18** UOR polarization curves of (B,P,Co,Fe)-Ni@PW at different reaction times.
- Fig. S19** HER polarization curves of (P,Co)-Ni@PW, P-Ni@PW, and (B,P,Co,Fe)-Ni@PW.
- Fig. S20** The Tafel slopes of (P,Co)-Ni@PW, (B,P,Fe)-Ni@PW, and (B,P,Co,Fe)-Ni@PW for HER.
- Fig. S21** The Tafel slopes of (P,Co)-Ni@PW, (B,P,Fe)-Ni@PW, and (B,P,Co,Fe)-Ni@PW for UOR.
- Fig. S22** CV curves of the (P,Co)-Ni@PW at different scan rates.
- Fig. S23** CV curves of the (B,P,Fe)-Ni@PW at different scan rates.
- Fig. S24** CV curves of the (B,P,Co,Fe)-Ni@PW at different scan rates.
- Fig. S25** Evaluated  $C_{dl}$  values of (P,Co)-Ni@PW, (B,P,Fe)-Ni@PW, and (B,P,Co,Fe)-Ni@PW.
- Fig. S26** SEM image of the (B,P,Co,Fe)-Ni@PW after cycle test for HER.
- Fig. S27** SEM image of the (B,P,Co,Fe)-Ni@PW after cycle test for UOR.
- Fig. S28** CV curves of the (B,P,Co,Fe)-Ni@PW after cycle.
- Fig. S29** The photo shows the initial state of the balloon in 1 M KOH + 0.33 M urea.
- Fig. S30** The photo shows the initial state of the balloon in 1 M KOH.
- Fig. S31** The photos showing the HER||OER and HER||UOR electrolyzer.
- Fig. S32** DFT-optimized structure model of the (a) P-Ni@PW, (b) (P,Co)-Ni@PW.
- Fig. S33** Charge density difference for (a) P-Ni@PW, (b) (P,Co)-Ni@PW.
- Fig. S34** Schematic illustration of the proposed UOR mechanisms.
- Table S1.** UOR performance comparison between (B,P,Co,Fe)-Ni@PW and recently reported UOR electrocatalysts in alkaline urea media.

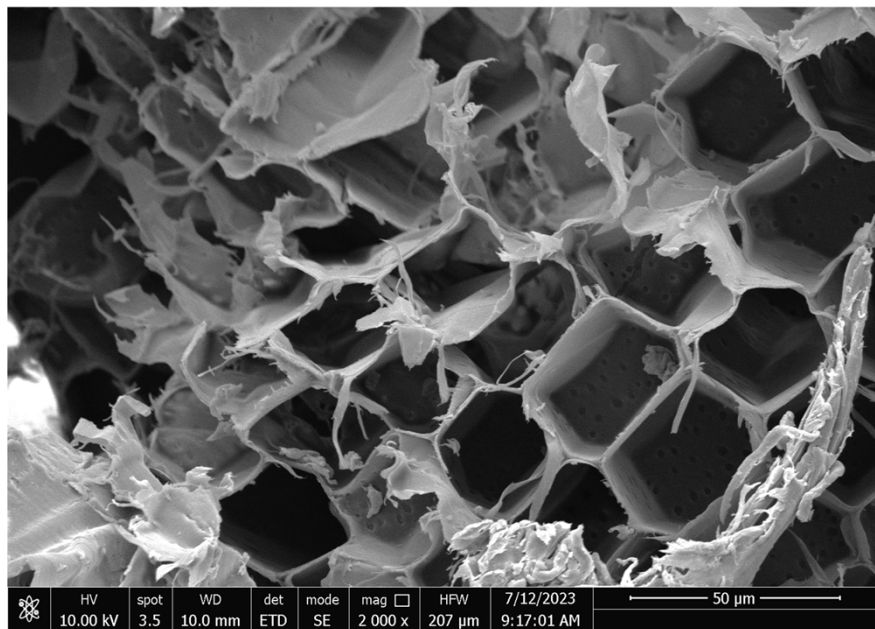


**Fig. S1** SEM image of the natural paulownia wood.

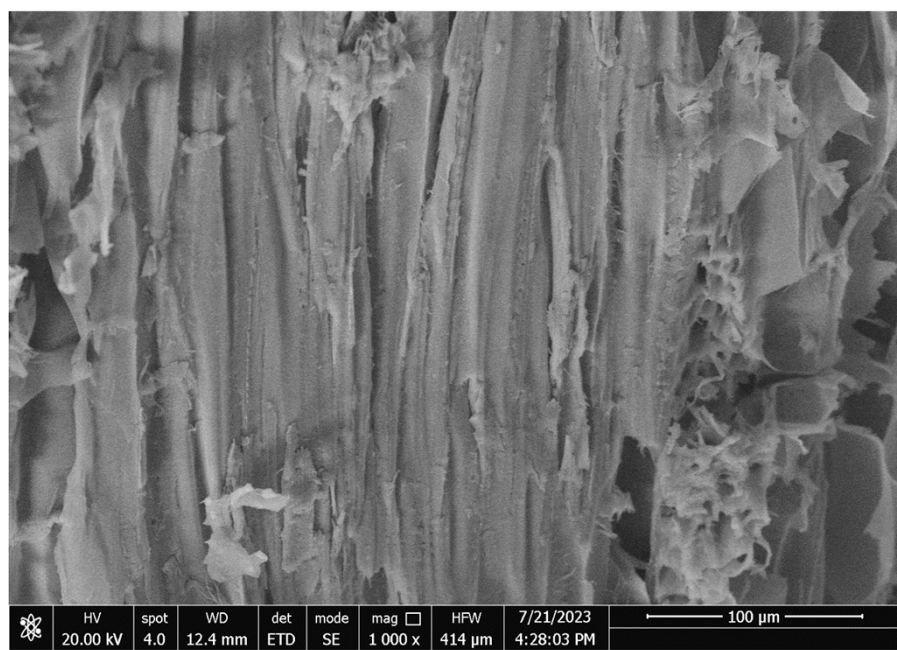


**Fig. S2** SEM images of the natural paulownia wood along the direction of tree growth.



**Fig. S3** The photo of the natural leave loaded with alloys.

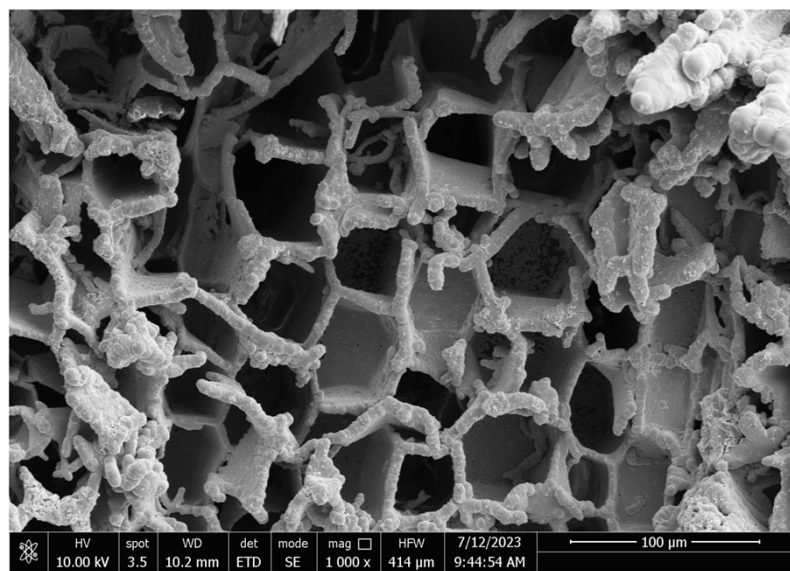


**Fig. S4** SEM images of the (B,P,Co,Fe)-Ni@PW.

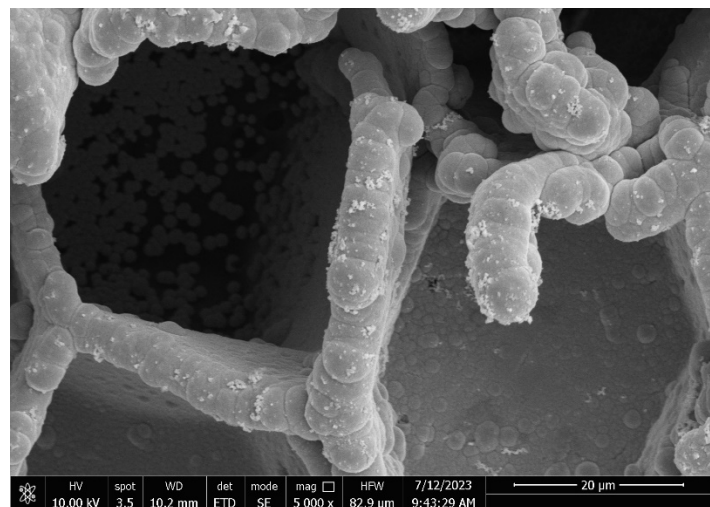


**Fig. S5** SEM images of the (B,P,Co,Fe)-Ni@PW.

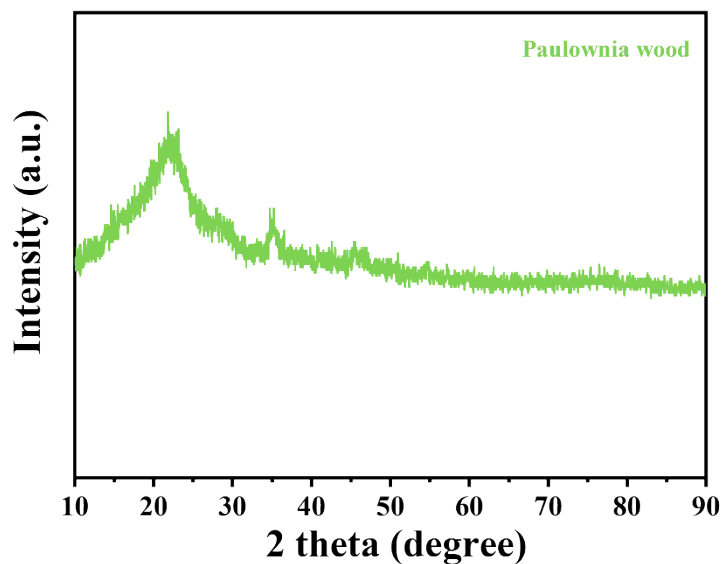


**Fig. S6** XRD pattern of PW.

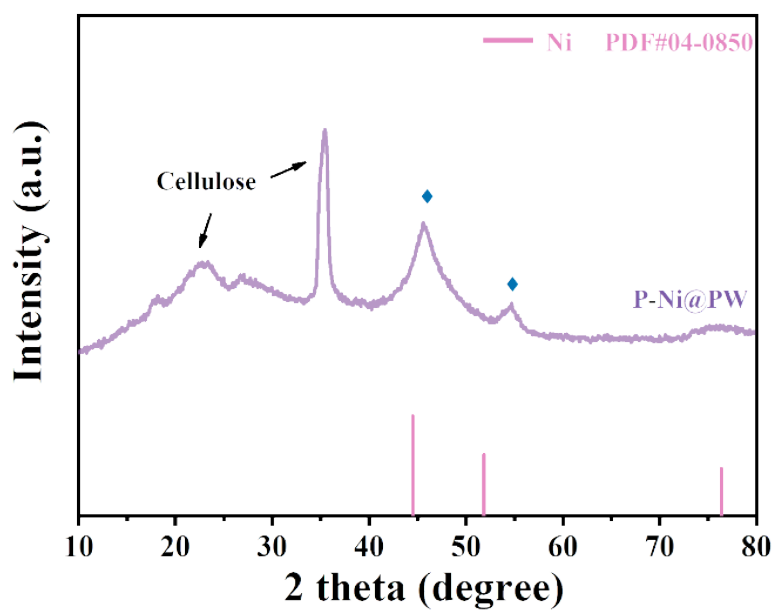


**Fig. S7** XRD pattern of P-Ni@PW.

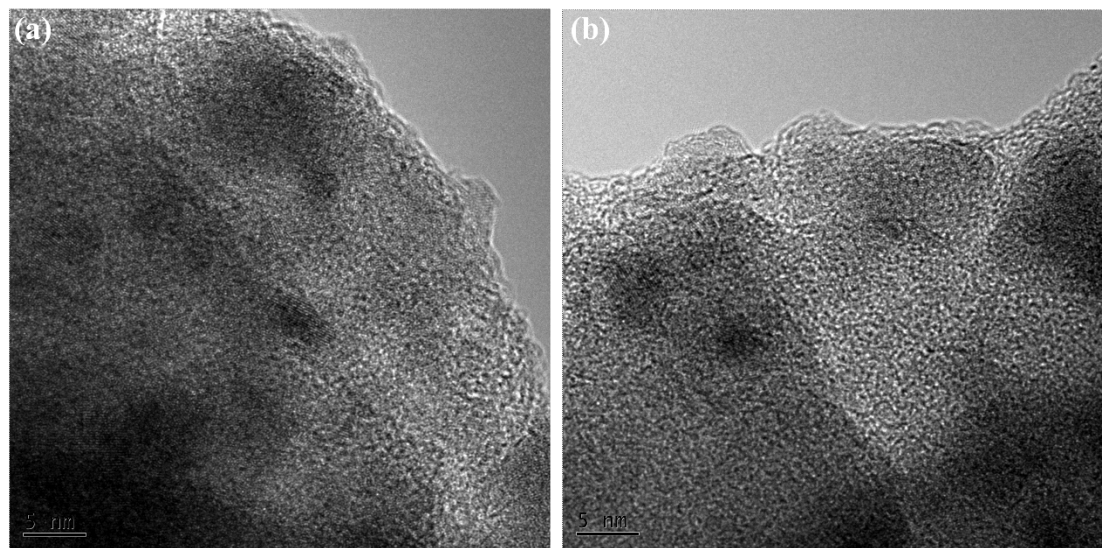


**Fig. S8** HRTEM images of the (B,P,Co,Fe)-Ni@PW.

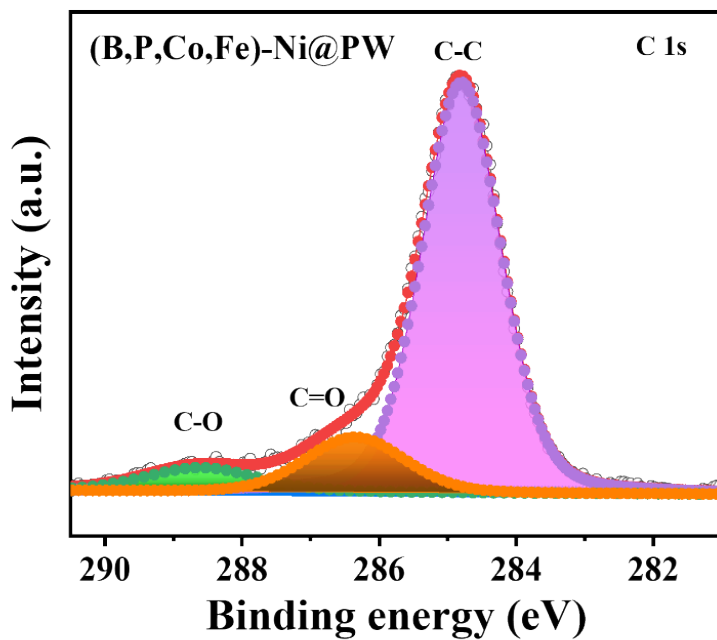


**Fig. S9** High-resolution XPS spectra of (B,P,Co,Fe)-Ni@PW for C 1s.

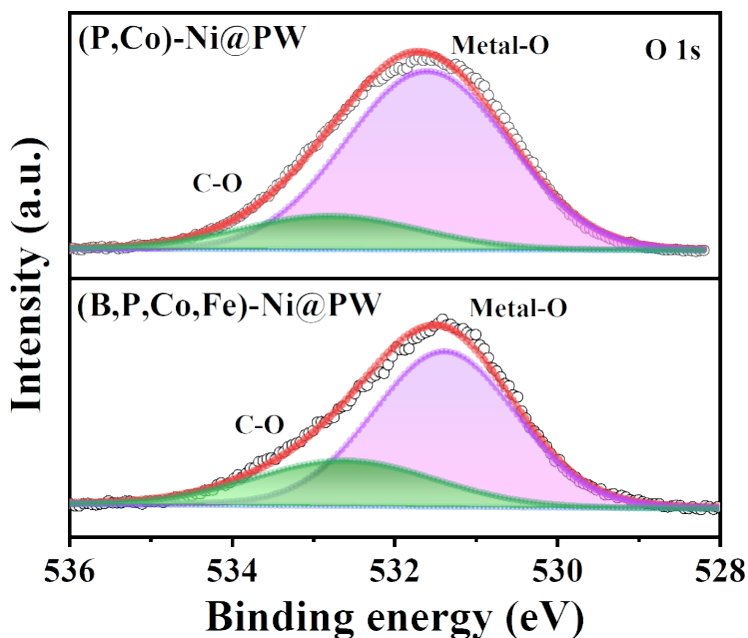


**Fig. S10** High-resolution XPS spectra of (P,Co)-Ni@PW and (B,P,Co,Fe)-Ni@PW for O 1s.

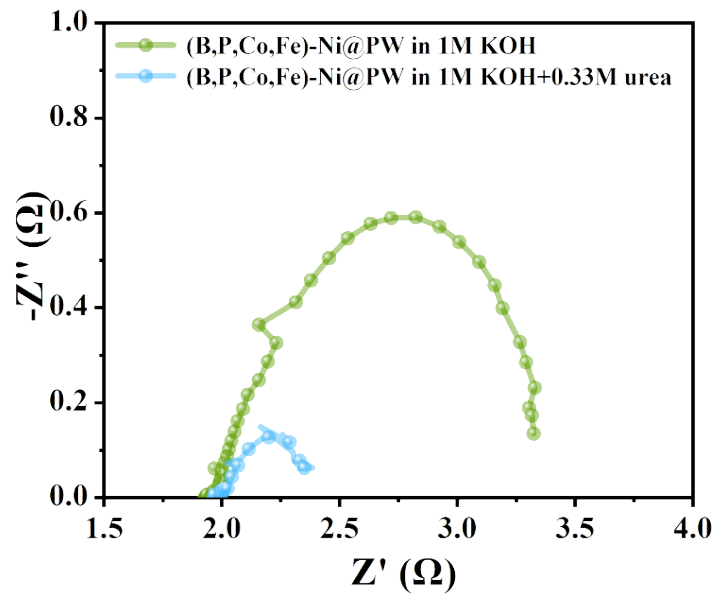


**Fig. S11** Nyquist plots of the (B,P,Co,Fe)-Ni@PW for OER and UOR.

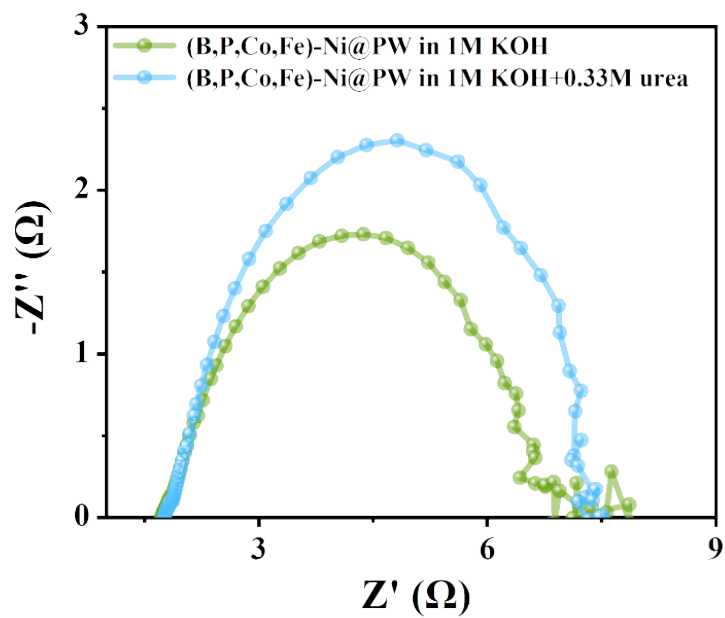


**Fig. S12** Nyquist plots of the (B,P,Co,Fe)-Ni@PW for HER in 1 M KOH with and without urea.

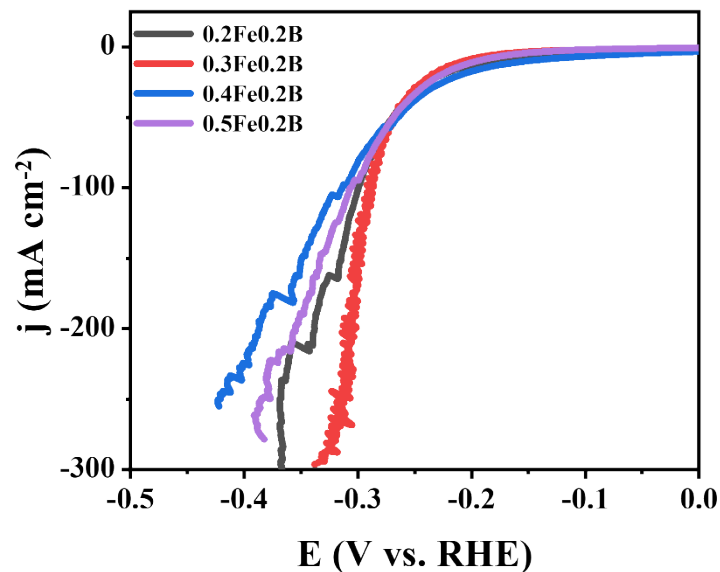


**Fig. S13** HER polarization curves of (B,P,Co,Fe)-Ni@PW with different mass ratios.

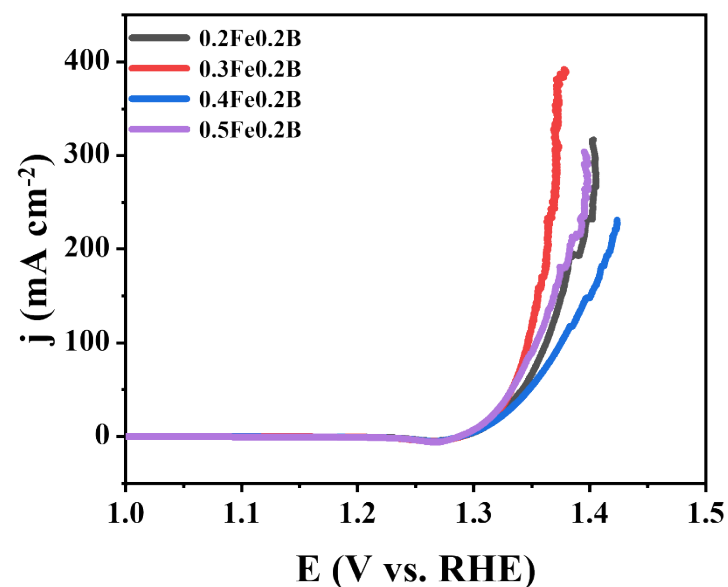


**Fig. S14** UOR polarization curves of (B,P,Co,Fe)-Ni@PW with different mass ratios.

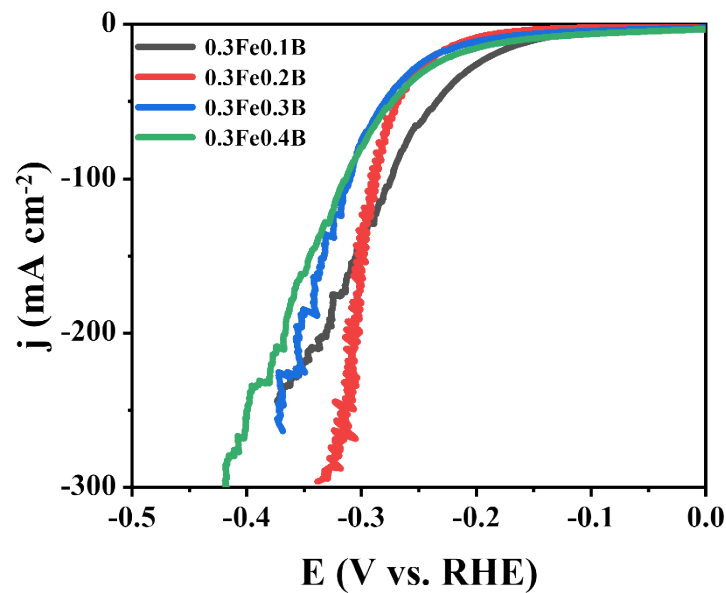


**Fig. S15** HER polarization curves of (B,P,Co,Fe)-Ni@PW with different mass ratios.

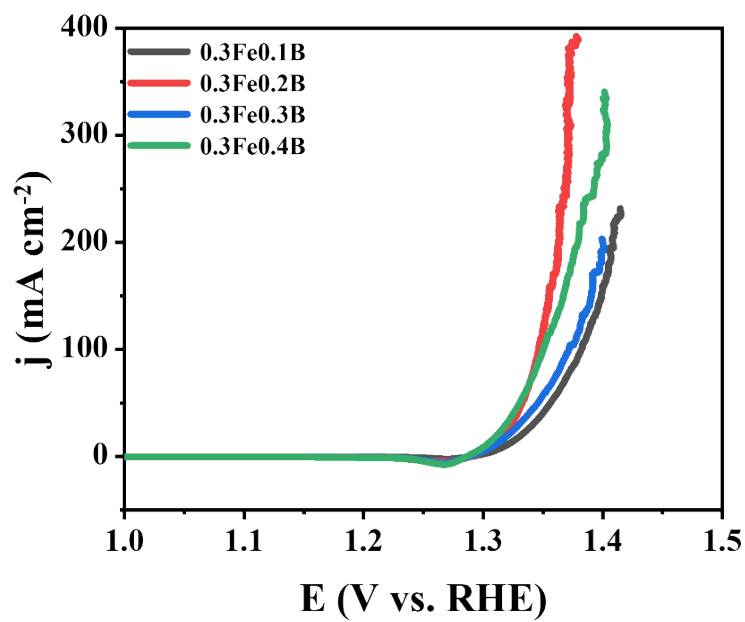


**Fig. S16** UOR polarization curves of (B,P,Co,Fe)-Ni@PW with different mass ratios.

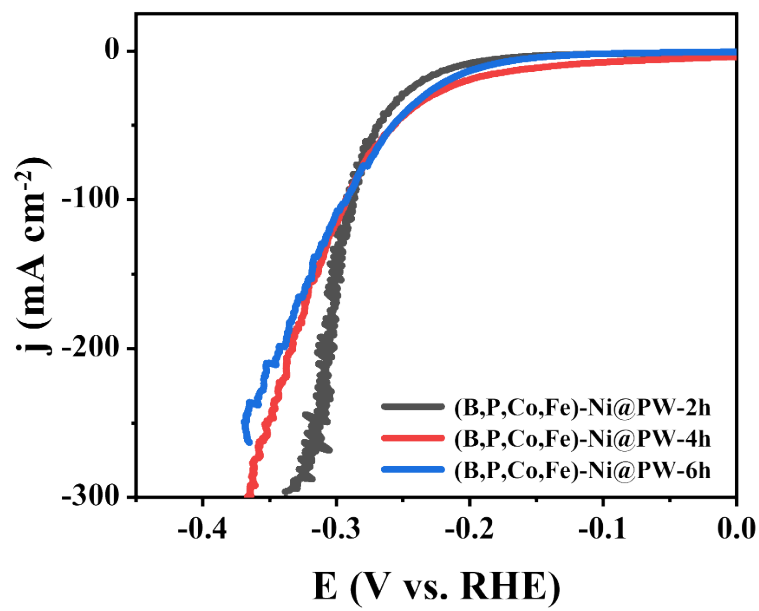


**Fig. S17** HER polarization curves of (B,P,Co,Fe)-Ni@PW at different reaction times.

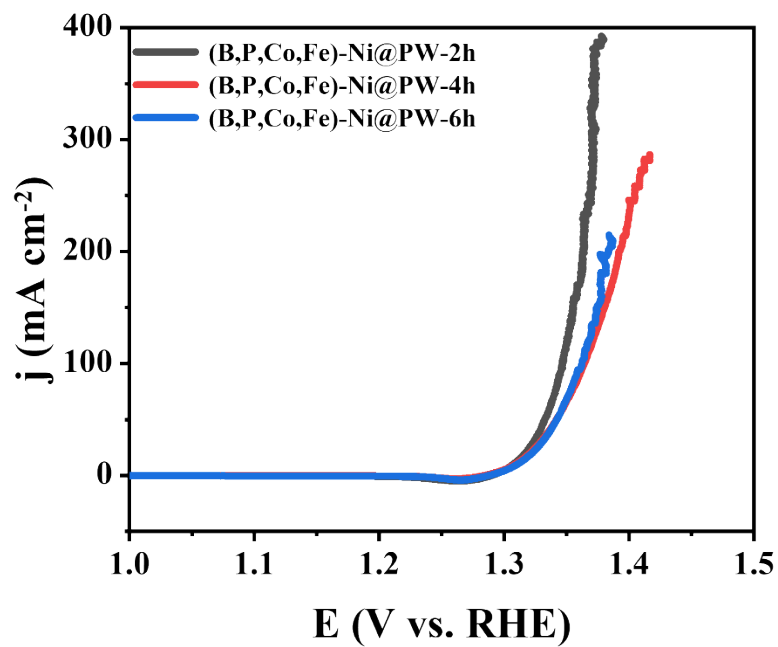


**Fig. S18** UOR polarization curves of (B,P,Co,Fe)-Ni@PW at different reaction times.

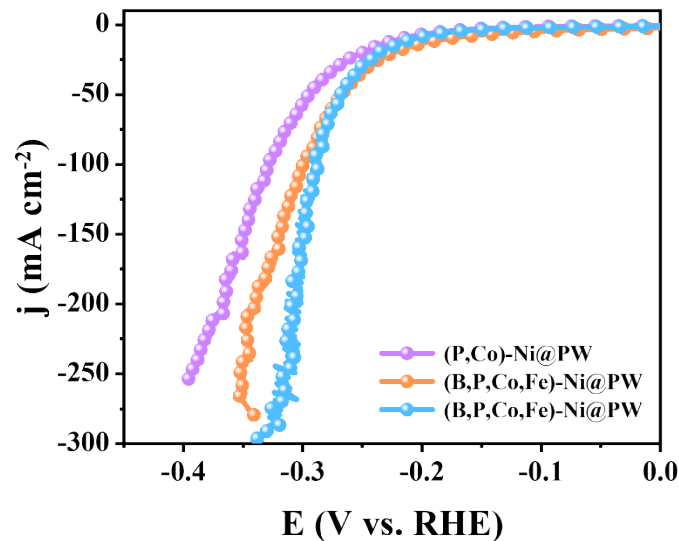


**Fig. S19** HER polarization curves of (P,Co)-Ni@PW, (B,P,Fe)-Ni@PW, and (B,P,Co,Fe)-Ni@PW.

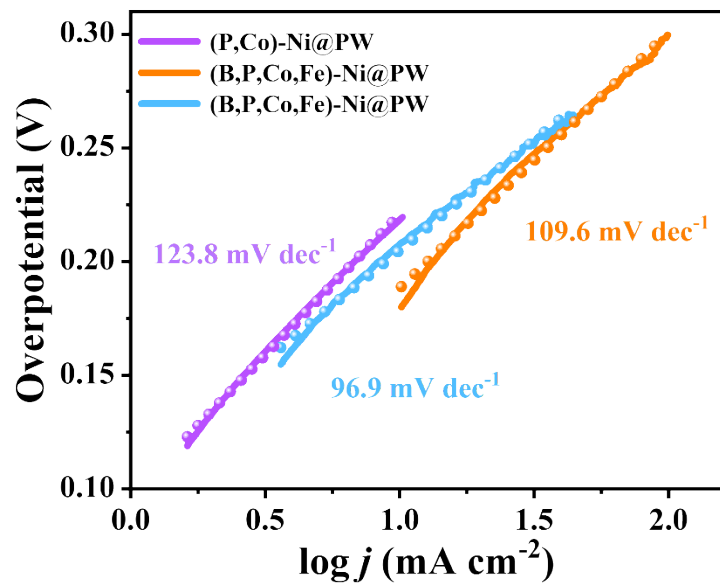


**Fig. S20** The Tafel slopes of (P,Co)-Ni@PW, (B,P,Fe)-Ni@PW, and (B,P,Co,Fe)-Ni@PW for HER.

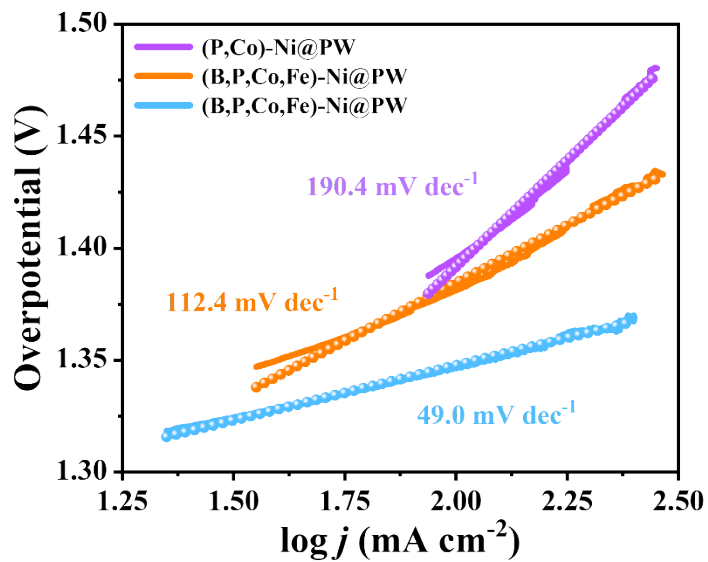


**Fig. S21** The Tafel slopes of (P,Co)-Ni@PW, (B,P,Fe)-Ni@PW, and (B,P,Co,Fe)-Ni@PW for UOR.

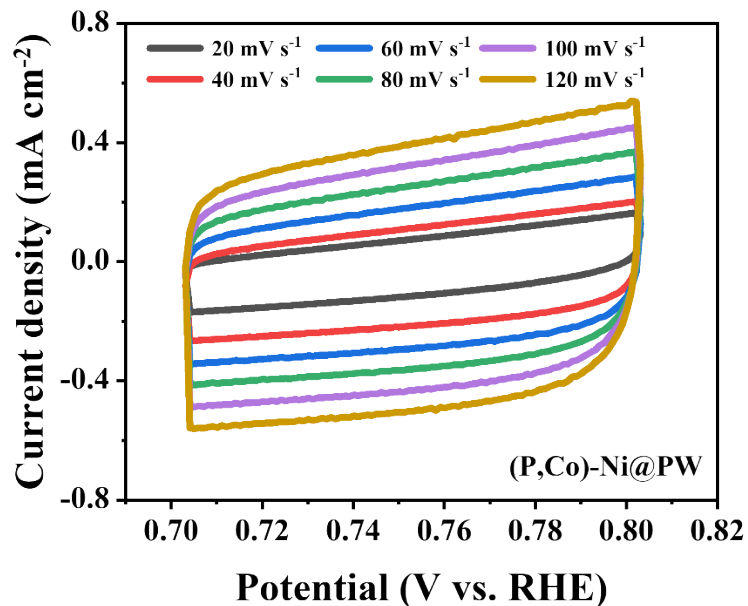


**Fig. S22** CV curves of the (P,Co)-Ni@PW at different scan rates.

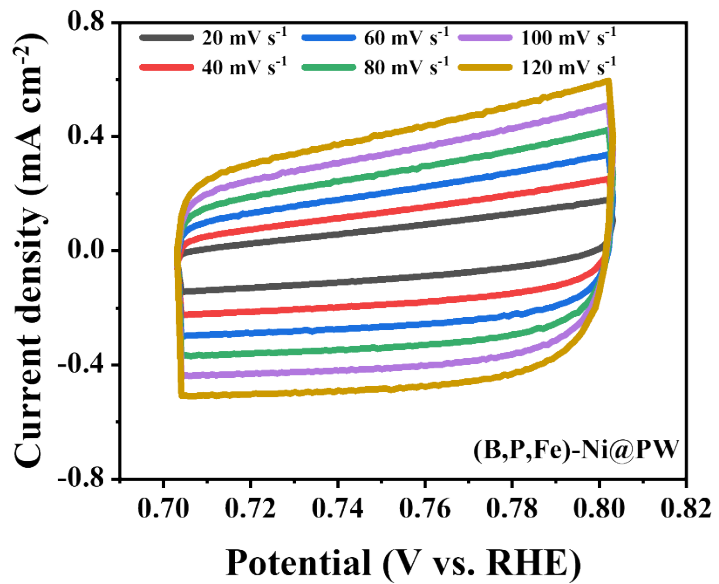


**Fig. S23** CV curves of the  $(\text{B},\text{P},\text{Fe})\text{-Ni@PW}$  at different scan rates.

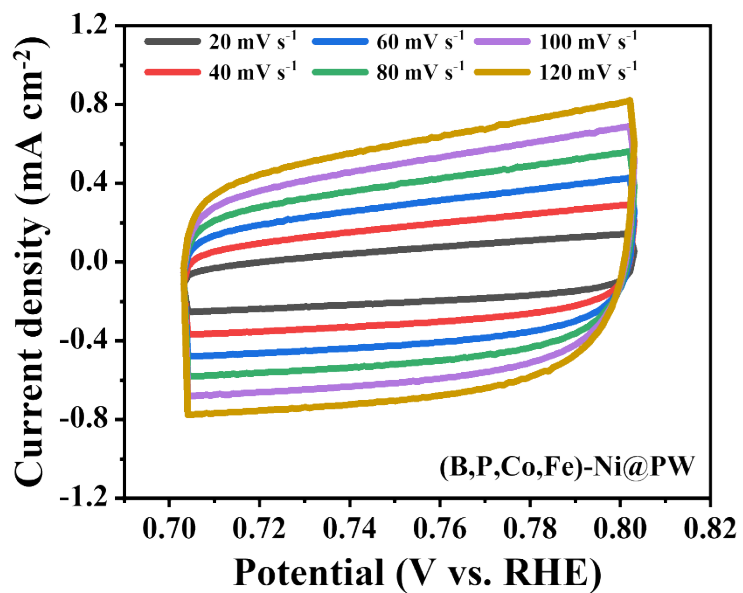


**Fig. S24** CV curves of the  $(\text{B},\text{P},\text{Co},\text{Fe})\text{-Ni@PW}$  at different scan rates.

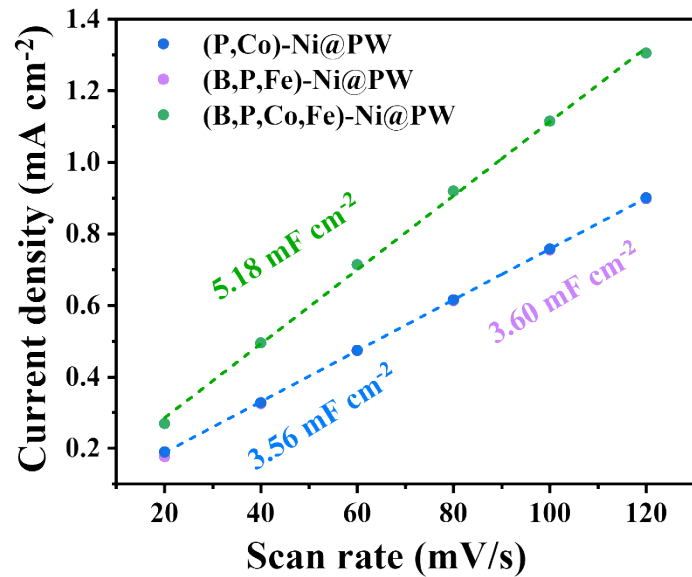


**Fig. S25** Evaluated  $C_{dl}$  values of (P,Co)-Ni@PW, (B,P,Fe)-Ni@PW, and (B,P,Co,Fe)-Ni@PW.

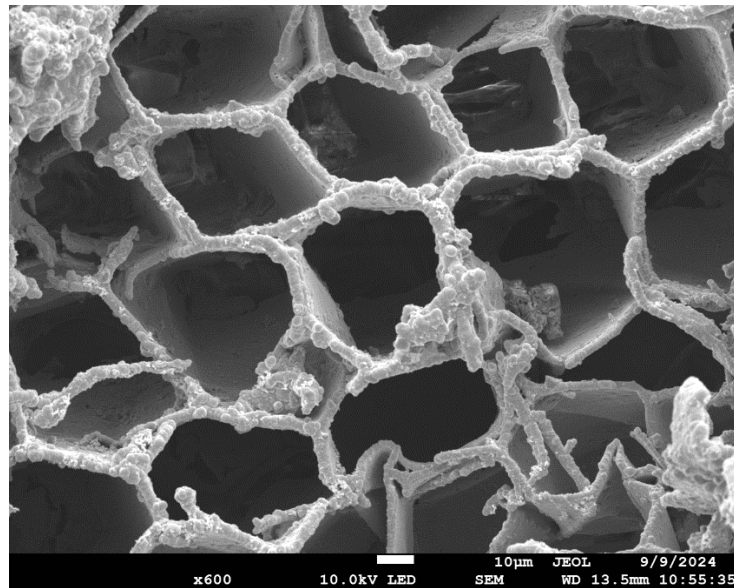


**Fig. S26** SEM image of the (B,P,Co,Fe)-Ni@PW after cycle test for HER.

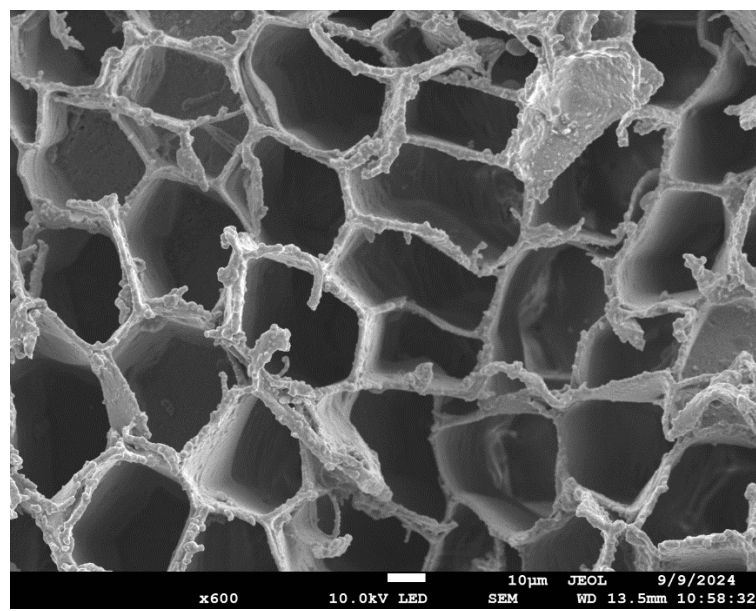


**Fig. S27** SEM image of the (B,P,Co,Fe)-Ni@PW after cycle test for UOR.

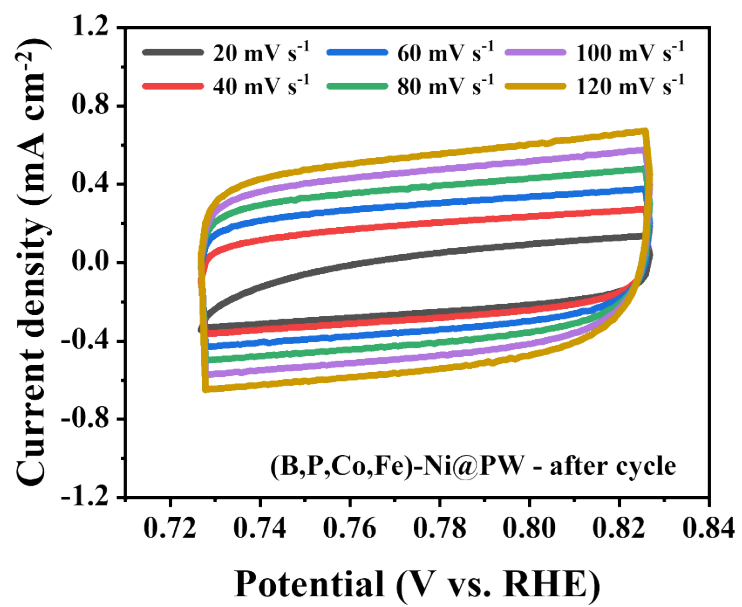


**Fig. S28** CV curves of the (B,P,Co,Fe)-Ni@PW after cycle.



**Fig. S29** The photo shows the initial state of the balloon in 1 M KOH + 0.33 M urea.



**Fig. S30** The photo shows the initial state of the balloon in 1 M KOH.

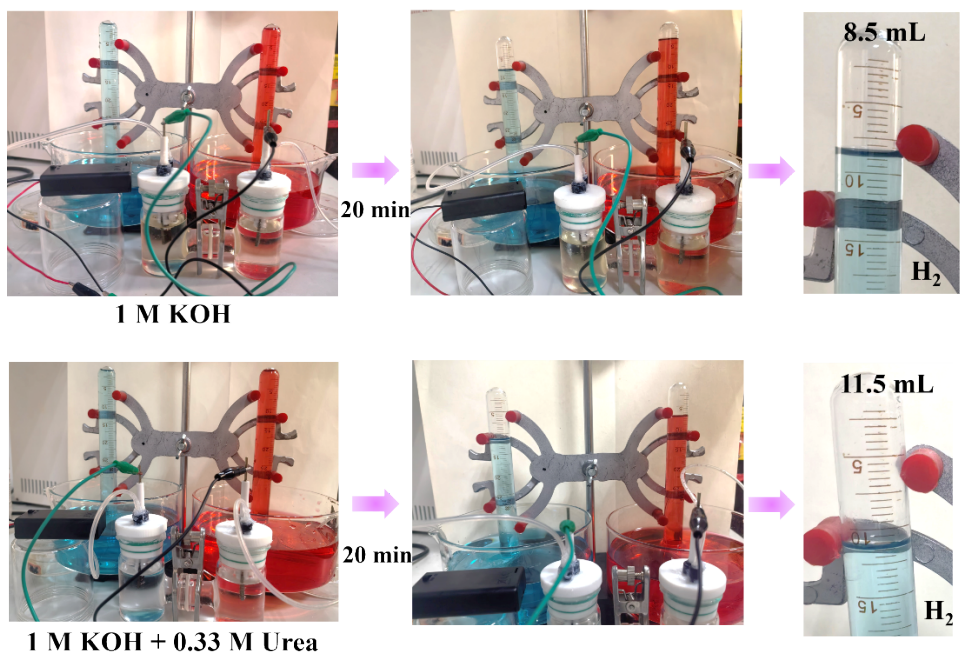


**Fig. S31** The photos showing the HER||OER and HER||UOR electrolyzer.

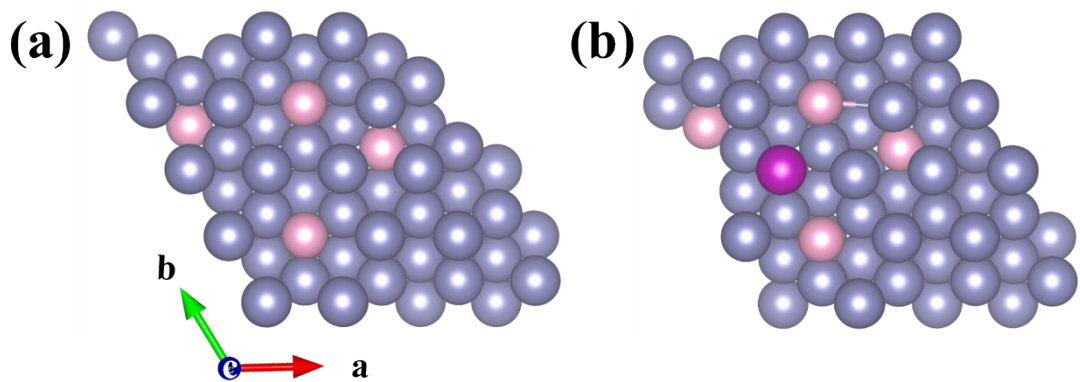


**Fig. S32** DFT-optimized structure model of the a) P-Ni@PW, b) (P,Co)-Ni@PW.

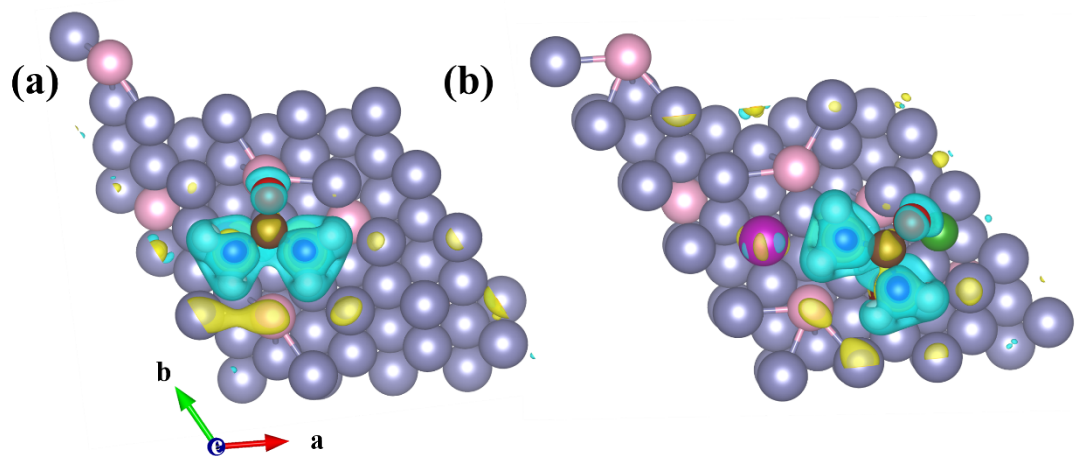


**Fig. S33** Charge density difference for a) P-Ni@PW, b) (P,Co)-Ni@PW.

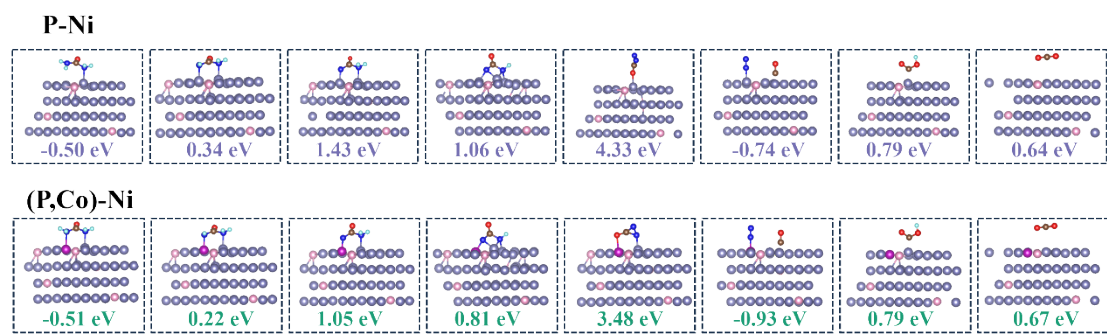


**Fig. S34** Schematic illustration of the proposed UOR mechanisms.

**Table S1.** UOR performance comparison between (B,P,Co,Fe)-Ni@PW and recently reported UOR electrocatalysts in alkaline urea media.

Electrocatalysts	Electrolyte	$\eta_{100}$ V	Refs
<b>(B,P,Co,Fe)-Ni@PW</b>	1 M KOH+0.33 M Urea	<b>1.34</b>	<b>This work</b>
Ni/W <sub>5</sub> N <sub>4</sub>	1 M KOH+0.5 M Urea	1.38	[S1]
hcp-CoNi-N/C	1 M KOH+0.33 M Urea	1.39	[S2]
Ni <sub>3</sub> /Mo <sub>2</sub> N	1 M KOH+0.33 M Urea	1.37	[S3]
NiCoGe	1 M KOH+0.33 M Urea	1.33	[S4]
O <sub>vac</sub> -NiOOH	1 M KOH+0.33 M Urea	1.47	[S5]
Fe-Ni <sub>3</sub> S <sub>2</sub>	1 M KOH+0.33 M Urea	1.50	[S6]
NiOOH/LDH/FeOOH	1 M KOH+0.33 M Urea	1.39	[S7]
Ni(OH) <sub>2</sub> /NF	1 M KOH+0.33 M Urea	1.45	[S8]
Ni-CuO/NF	1 M KOH+0.33 M Urea	1.36	[S9]
Ni-TPA@ NiSe/NF	1 M KOH+0.33 M Urea	1.37	[S10]

## References

- [S1] H. Sun, J. Liu, H. Kim, S. Song, L. Fei, Z. Hu, H. J. Lin, C. T. Chen, F. Ciucci and W. Jung, *Adv. Sci.*, 2022, **9**, 2204800.
- [S2] Y. Zhou, B. Chu, Z. Sun, L. Dong, F. Wang, B. Li, M. Fan and Z. Chen, *Appl. Catal. B Environ.*, 2023, **323**, 122168.
- [S3] P. Wang, X. Bai, H. Jin, X. Gao, K. Davey, Y. Zheng, Y. Jiao and S. Z. Qiao, *Adv. Funct. Mater.*, 2023, **33**, 2300687.
- [S4] T. Wang, L. Miao, S. Zheng, H. Qin, X. Cao, L. Yang and L. Jiao, *ACS Catal.*, 2023, **13**, 4091-4100.
- [S5] L. Jin, R. Ji, H. Wan, J. He, P. Gu, H. Lin, Q. Xu and J. Lu, *ACS Catal.*, 2023, **13**, 837-847.
- [S6] M. Cai, Q. Zhu, X. Wang, Z. Shao, L. Yao, H. Zeng, X. Wu, J. Chen, K. Huang and S. Feng, *Adv. Mater.*, 2022, **35**, 2209338.
- [S7] D. Li, W. Wan, Z. Wang, H. Wu, S. Wu, T. Jiang, G. Cai, C. Jiang and F. Ren, *Adv. Energy Mater.*, 2022, **12**, 2201913.
- [S8] P. Li, Y. Huang, X. Ouyang, W. Li, F. Li and S. Tian, *Chem. Eng. J.*, 2023, **464**, 142570.
- [S9] H. Qin, Y. Ye, J. Li, W. Jia, S. Zheng, X. Cao, G. Lin and L. Jiao, *Adv. Funct. Mater.*, 2022, **33**, 2209698.
- [S10] S. W. Tatarchuk, J. J. Medvedev, F. Li, Y. Tobolovskaya and A. Klinkova, *Angew. Chem., Int. Ed.*, 2022, **61**, e202209839.